

RESEARCH ARTICLE

A consensus layer V pyramidal neuron can sustain interpulse-interval coding

Chandan Singh, William B. Levy*

Departments of Neurosurgery and of Psychology, University of Virginia, Charlottesville, VA, United States of America

* wbl@virginia.edu



Abstract

In terms of a single neuron's long-distance communication, interpulse intervals (IPIs) are an attractive alternative to rate and binary codes. As a proxy for an IPI, a neuron's time-to-spike can be found in the biophysical and experimental intracellular literature. Using the current, consensus layer V pyramidal neuron, the present study examines the feasibility of IPI-coding and examines the noise sources that limit the information rate of such an encoding. In descending order of importance, the noise sources are (i) synaptic variability, (ii) sodium channel shot-noise, followed by (iii) thermal noise. The biophysical simulations allow the calculation of mutual information, which is about 3.0 bits/spike. More importantly, while, by any conventional definition, the biophysical model is highly nonlinear, the underlying function that relates input intensity to the defined output variable is linear. When one assumes the perspective of a neuron coding via first hitting-time, this result justifies a pervasive and simplifying assumption of computational modelers—that a class of cortical neurons can be treated as linearly additive, computational devices.

OPEN ACCESS

Citation: Singh C, Levy WB (2017) A consensus layer V pyramidal neuron can sustain interpulse-interval coding. PLoS ONE 12(7): e0180839. <https://doi.org/10.1371/journal.pone.0180839>

Editor: Miguel Maravall, University of Sussex, UNITED KINGDOM

Received: January 31, 2017

Accepted: June 22, 2017

Published: July 13, 2017

Copyright: © 2017 Singh, Levy. This is an open access article distributed under the terms of the [Creative Commons Attribution License](https://creativecommons.org/licenses/by/4.0/), which permits unrestricted use, distribution, and reproduction in any medium, provided the original author and source are credited.

Data Availability Statement: All data files are available from the figshare database (doi [10.6084/m9.figshare.3858342](https://doi.org/10.6084/m9.figshare.3858342)).

Funding: We thank the Department of Neurosurgery for their financial support and also are thankful for the US National Science Foundation Grant 1162449. The funders had no role in study design, data collection and analysis, decision to publish, or preparation of the manuscript.

Competing interests: The authors have declared that no competing interests exist.

Introduction

This study addresses three contemporary topics that are part of understanding neural computation and neural codes: (1) Is there a cortical neuron whose output is consistent with the assumption of linear additivity? (2) What are the relative contributions of the stochastic processes that limit information flow through a neuron? And (3) what is the mutual information, bits-per-spike, for such a neocortical pyramidal cell?

McCulloch and Pitts [1] introduce the computational neuron as a deterministic threshold-linear device. Gerstein and Mandelbrot [2] consider a linearly additive neuron in a stochastic setting (their “random walk model”). However, even in this novel work, which assumes a linearly additive neuron, there is the absence of whole-hearted support for such additivity because of a neuron's known leak-currents. Indeed, although there has been some biophysical modeling that attempts to justify a linear neuron [3–5], much more effort has gone into understanding the stochastic, leaky-neuron model [6–13]. The focus here is motivated by interpulse interval (IPI) coding since it has the highest bit-rate possible of any code using constant-amplitude pulses [14–17] (proof: if there is no information in amplitude, all information must

be in interpulse intervals. A code that retains the value of every interpulse interval loses no information). Moreover, for fixed-amplitude pulses and fixed and axonal leak rates that are suitably more expensive than a pulse, no code is more energy efficient in terms of bits / joule than IPI coding.

Any spike-generating neuron is, fundamentally, non-linear with much research aimed at understanding such non-linear behavior. Such research includes identifying differential equations that reproduce observed firing patterns (e.g., [18–20]). Our perspective asks a different question: Is there a cortical neuron whose output—time-to-spike (TTS) from rest to spike generation—is consistent with the assumption of linear additivity of synaptic excitation? By linear additivity we mean that the TTS is inversely directly proportional to the synaptic intensity. To achieve such linearity clearly requires an underlying nonlinear model since both the RC-leak of a neuron and the driving voltage of synaptic excitation cause sublinearity of the net synaptic effects.

Beginning with certain empirical studies, there is progressively stronger motivation for considering a physiological, functioning pyramidal neuron of the cortex to be a linearly additive computational device. The work of Ferster [21–24] and follow-up research [25–27] stands out in this regard because of the use of intracellular recording in perceptually relevant situations. Other intracellular work supports the existence of linearly additive voltage-ranges [28–31]. However, it is easy to find references to non-linear behavior that includes sublinear and supra-linear [31, 32]. But in choosing one's motivation, we come down on the side of intracellular observations in awake behaving organisms as the greatest relevance.

Beyond such empirical literature, there is the computational and code-theoretic literature that implicitly assume some kind of linear excitation function. The two, non-mutually exclusive positions are a population-coding conjecture [33–39] and a single neuron Bayesian computational conjecture [40–45]. Implicitly or explicitly, such theoretical stances assume that a neuron's appropriate range of operation is characterized by linear additivity of its synaptic input events.

Running against this trend for linear additivity, there is a long history of biophysical analyses beginning with Stein [12] and continuing up to the present day, with more complicated models (e.g. the Hodgkin-Huxley model of [13] and the QIF model of [20]). In purely passive models, a neuron's behavior between resting potential and spike-threshold is subadditive in excitation. In models with leak and voltage-dependency, there can be subadditivity, superadditivity, or both. In any case, there is a path dependency (voltage as a function of time); this dependency prevents the exact inversion of first hitting-time (time to reach threshold) into input intensity. That is, the first hitting-time for an RC-leaky neuron, or more complicated models built on top of an RC-leaky neuron, cannot be properly inverted into the average intensity of net synaptic excitation for any one, specific IPI; although one could claim the average path is good enough, we do not pursue this option as it surely loses information.

The focus here is on one particular recent biophysical model culminating in [46]; this model reproduces action potential shape and firing found in empirical studies. This model of a layer V pyramidal neuron of cerebral cortex is published as non-stochastic and is selected because it seems to be the “consensus pyramidal neuron” with several labs using the same model morphology [19, 47–49] and not infrequently the same voltage-activated conductances (VGCs) [50], and even some agreeing in terms of the varieties and placements of VGCs [46, 49, 51, 52]. The VGCs present in these models include, two voltage-controlled K-channels (a delayed rectifier and a K_A -type) and two types of voltage-controlled Na-channels (Nav 1.2 and Nav 1.6) with a specific microscopic distribution, notably a high concentration of the low-threshold Nav 1.6 channels in the axonal initial segment (AIS) [46, 52–55].

Here, the deterministic model (continuous Na-channel conductances as a function of voltage) is the starting point. For both deterministic and stochastic intensities, the relationship between injected current and TTS is quantified by relating input intensity to inverse TTS. The results suggest that, for the neocortical neuron studied here whose underlying biophysics are non-linear, a linearly additive model well-approximates the input-output behavior over a range of excitatory intensities. Using the inverse linear relationship for decoding, the model is then used to evaluate noise or noise-like effects. Three noise or noise-like processes are considered—thermal, Na-channel shots, and random synaptic arrivals; synaptic arrivals are, by far, the dominant noise-source. Here, Shannon’s mutual information measures information transmission; the channel input is a randomly chosen, scalar latent variable that parameterizes the Poisson intensity of the totality of the synaptic activations, and the output variable is 1/TTS. The estimate of this mutual information is approximately 3.0 bits per spike.

Results

The results here begin with examples that show inverse TSS is linearly related to input intensity. This inverse linearization motivates the assumption of an inverse Gaussian, first hitting-time probability-distribution. This hypothesis leads to (i) an examination of the statistical distribution of TTS and (ii) a comparison of the contribution of three physical sources of randomization that affect the variance of this first-hitting time distribution. Finally, with the assumption of a prior distribution, mutual information of a defined neural computation can be calculated.

Linearized inverse time-to-spike

The model sustains an inverse linear range for current-steps ranging from 0.51 nA to 0.85 nA when there is the requirement that action potential initiation begins at the AIS; relaxing this last requirement slightly extends the range (the upper bound becomes 1.0 nA). Fig 1 illustrates this inverse relationship. Fig 1A uses the point-injection of a current-step. the slope is $0.30 \mu\text{C}^{-1}$ with an extrapolated y-intercept at zero-current of -0.13 ms^{-1} . Spatially-distributed, synaptic activation (with an input intensity rate λ) also has the linear relationship; here, the slope is

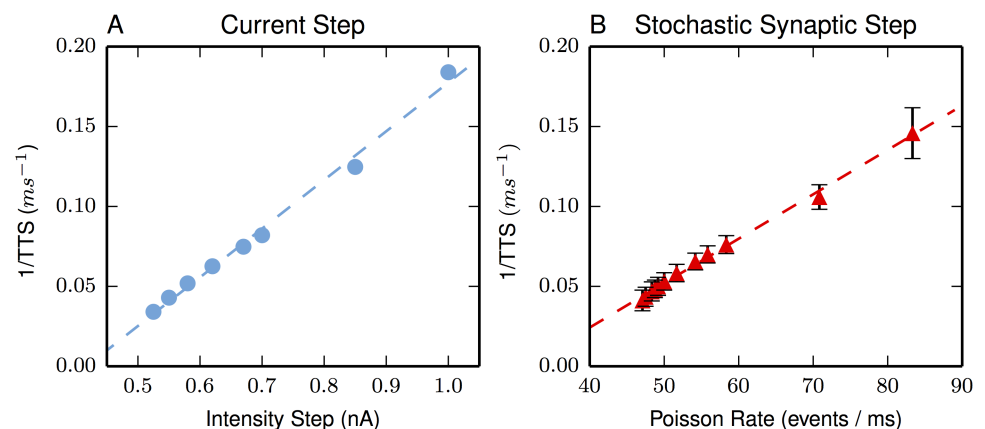


Fig 1. Inverse TTS approximates a linear function of excitation. Excitation is either (A) a point dendritic current-step or (B) a spatially dispersed, synaptic activation. Lines are best linear fits (see text). Each point is an average of 120 excitations from rest. The error bars (SEM) for the current-step are within the plot points. All points but the highest intensities always had spike initiation at the AIS. At the largest intensity on each curve, the spike originated in the dendrite 20 percent of the time.

<https://doi.org/10.1371/journal.pone.0180839.g001>

0.0028 events⁻¹ with a zero-intensity intercept of -0.09 ms⁻¹. Perhaps due to the spatially distributed nature of synaptic activation, the currents required to induce a spike are consistently larger than the currents delivered by point-current injections. For example, the rate of synaptic activation needed to achieve a 1 nA spatially distributed current injection is 83.3 events/ms (assuming a 50 mV driving potential, 200 pS / synapse, and a synaptic event duration of 1.2 ms). By comparison, for the same net current injection, 1/TTS for the point injection is 0.18 while it is 0.14 for the spatially distributed synaptic current.

Variation in TTS

The overriding variation of the TTS using synaptic activation arises from the variability of the stochastic process itself. This conclusion is best seen by comparing the deterministically generated TTSs against the stochastic synaptically generated TTSs, both with stochastic sodium channels.

For the highest intensities, the ratio of the variances is more than 200, while for the lowest intensities the ratio of the variances is more than 40. The standard deviations are plotted in Fig 2 for better visualization of the size of this effect as a function of inverse intensity (note that when viewing these curves, the leftmost values of TTS correspond to the highest intensities). The sodium channel shot-noise increases as the TTS increases; this shot-noise increase is mainly due to the number of events needed to fire a spike; i.e., threshold rises as TTS increases. Such a requirement for a greater amount of depolarization means that more sodium channels need to be activated to evoke an action potential. This larger number of sodium channels correlates with a larger standard deviation of TTS. Nevertheless, there is no spontaneous firing in this neuron; the contribution of an individual channel shot is not enough to fire the neuron until the neuron is very close to threshold.

As is well-known for additive point processes, a larger number of events with smaller values (conductances) leads to lower average variance of the steady-state voltage. This lower variance in the voltage is reflected as lower variance in the TTS. A simple model of this relationship between steady-state variance of the voltage and the variance of the TTS (as a first hitting-time

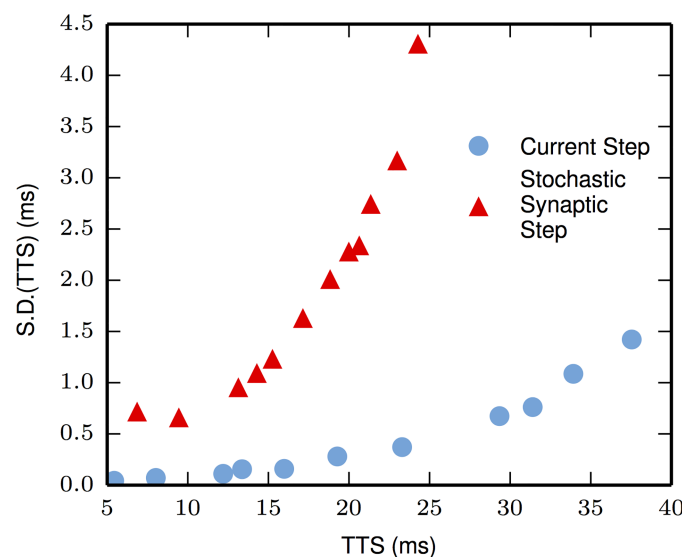


Fig 2. Synaptic activation increases variation. The only variation in TTS using a current-step is due to the stochastic nature of Na-channel activation. Random synaptic activation greatly increases the variation in TTS. Plot points, left-to-right, correspond to the reverse-ordered successive intensities of Fig 1.

<https://doi.org/10.1371/journal.pone.0180839.g002>

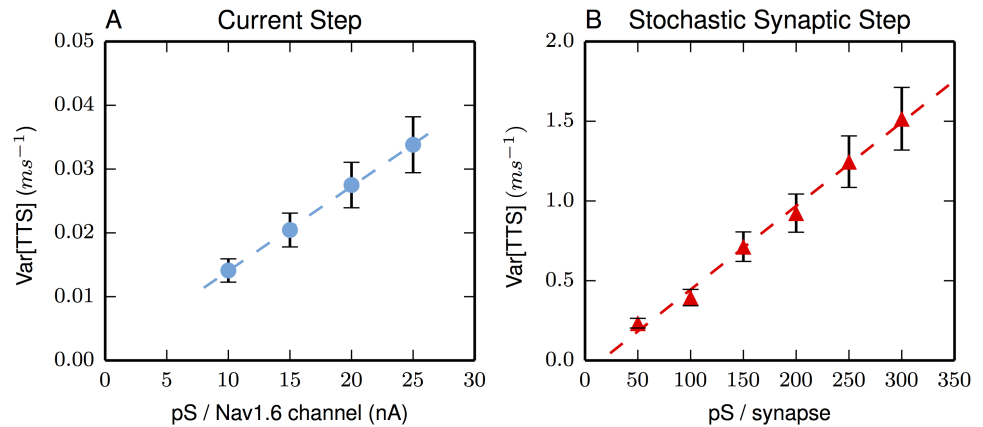


Fig 3. Synaptic shot-noise far exceeds Na-channel shot-noise. Random synaptic activation greatly increases the variation in TTS. (A) The only variation in TTS using a current-step is due to the stochastic nature of Na-channel activation. TTS variance increases as individual Na-channel conductance events get larger while keeping \bar{g} constant. By comparison in (B), the synaptic conductance events create much more variance. Note the y-axis scale differences. A current-step of 0.7 nA generates the data of (A). In (B), stochastic activation for each point is on average the same with a total conductance of 16.6 nS. Error bars are SEM. Lines are best linear fits (see text).

<https://doi.org/10.1371/journal.pone.0180839.g003>

distribution) is seen in the standard result [56] that the variances of a first hitting-time and of a Brownian motion (which shot noises can approximate) are proportional.

As one would expect, maintaining a constant total conductance (\bar{g}) while changing the pS/event changes the variance. In fact, there is a linear relationship between the size of the individual conductance event and the variance (see Fig 3). The best linear fit for Fig 3A is $\text{Var}[\text{TTS}] = 0.0012 \cdot x + 0.003$ with an R^2 value of 0.984 and the fit for Fig 3B is $\text{Var}[\text{TTS}] = 0.0052 \cdot x - 0.0797$ with an R^2 value of 0.993. The conductance of a sodium channel is in the vicinity of 10 – 20 pS [57–59], while the conductance of a synapse might average around 200 pS. Synaptic noise dominates, even when varying the parameters of the model (e.g. pS/channel, pS/synapse). When combining both sources of noise, the total noise is essentially indistinguishable from the noise generated solely by the synaptic input.

Finally, as will be important in the next section, it is necessary to have reliable probability distributions for the relationship between intensity and TTS. Fig 4 again shows that synaptic variation swamps sodium channel-induced variation (whatever noise is produced in the

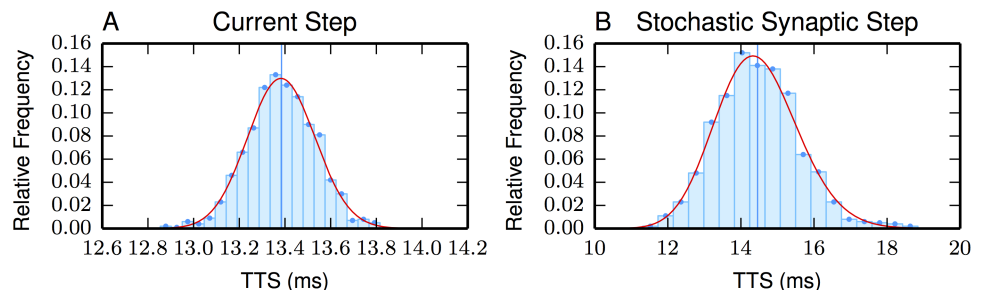


Fig 4. TTS relative frequency histogram and overlaid inverse Gaussian distribution with the same mean and variance. (A) is generated by a current-step of 0.67 nA, the mean TTS is 13.38 ms (vertical line) and the variance is 0.022 ms^2 . (B) is generated by Poisson synaptic activation ($\lambda = 55.8 \text{ events/ms}$), the mean TTS is 14.46 ms (vertical line) and the variance is 1.25 ms^2 . One thousand simulations produce each of the histograms. Current and synaptic activations begin at TTS = 0. Notice the x-axis scale difference.

<https://doi.org/10.1371/journal.pone.0180839.g004>

current-step histogram in Fig 4A will be biophysically added into the stochastic synaptic step histogram in Fig 4B). However, more to the point is that the TTS distribution can be fit by an inverse Gaussian distribution (see Fig 4).

Thermal noise

Thermal noise is also present, but it is the noise source of least concern. Although thermal noise increases with increasing resistance, the low-pass property of a resistive-capacitive circuit when recording across the capacitor exactly cancels out the resistance effect by lowering the high-frequency cutoff of the filter [60]. Thus, the thermal noise (calculated as the expected value of the variance of the voltage) is equal to $kT/C = 1.78 \times 10^{-11} \text{ V}^2$ (C is the capacitance of the neuron, 240 pF; k is the Boltzmann constant; and T is body temperature, 310 K). Thus, the standard deviation of this zero-centered noise is 4.22 μV . Compare this value to the shot noise fluctuations shown in Fig 5 inset; it is much smaller than the sodium channel shot-noise.

Mutual information, $I(\Lambda; \text{TTS})$

Treating the neuron as an information channel and as performing an experiment that estimates the value of Λ [61], the input-output variables are Λ and TTS, respectively. A proper calculation requires an appropriate range for both of these random variables. As in the fit to the histogram (Fig 4), the assumed range of TTS is the positive real line; however, as one can see in Fig 4, the probability of long and short durations is miniscule. Even though the earlier results demonstrate an expanded range for the intensities of synaptic activation beyond those reported by Hu et al, these ranges seem overly modest for a pyramidal neuron of neocortex whose average activity is under 10 Hz, implying the existence of firing times between a pair of pulses can be more than 100 ms. Regardless of the biophysical shortcomings of the model, an appropriate approximation for a meaningful mutual information requires one to extend the

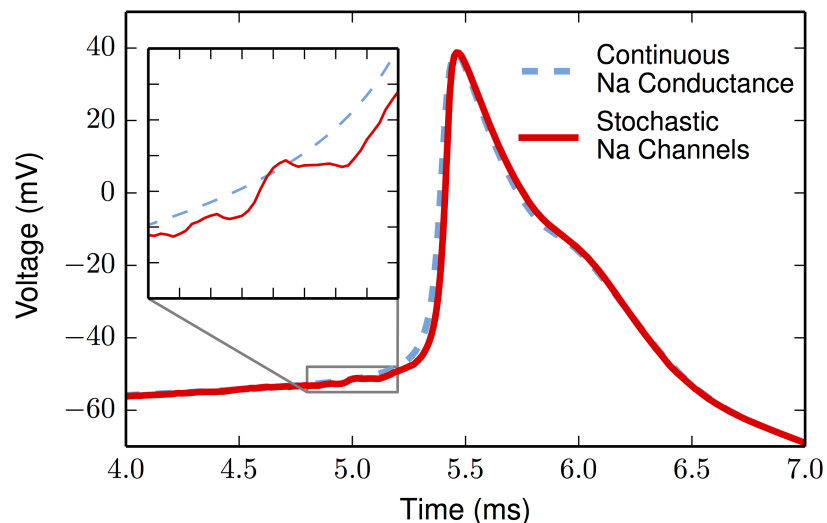


Fig 5. Comparison of a stochastic- and a deterministic-based action potential. The deterministic action potential (blue dashed line) reproduces the result of Hu et al; their action potential initiates at the AIS and spreads to the soma and apical dendrite. Aligned, peaked to peak, is a second action potential (solid red line) using stochastic Na-channels (both Nav 1.2 and Nav 1.6). Both action potentials are generated by the same somatic current-step of 1 nA. Inset y-axis goes from -55 mV to -48 mV (increments of 1 mV); inset x-axis goes from 4.8 ms to 5.2 ms (increments of 0.05 ms).

<https://doi.org/10.1371/journal.pone.0180839.g005>

Table 1. Distributions for Λ and associated mutual information values.

Distributional Form	Distribution	$E[\Lambda]$ (events/ms)	Mutual Information (bits/spike)
c/λ (see [45])	$1.07/\lambda$	54.2	3.00
c (Uniform)	0.020	58.1	2.77
$\frac{c \exp(-\lambda/c)}{c \exp(-\lambda_{min}/c) - \exp(-\lambda_{max}/c)}$	$\frac{\exp(-\lambda/100)}{28.59}$	55.9	2.99

Common to all distributions is the range of Λ : $\lambda \in [32.8, 83.3]$ events/ms. For each distribution, there is a different value of c to achieve normalization.

<https://doi.org/10.1371/journal.pone.0180839.t001>

range of synaptic intensities beyond those values appearing in Fig 1. Therefore, we extended the range on the low-intensity end to 200 ms. In this case, the mutual information is *c.a.* 20% larger than the model with the lesser range. (see S1 Fig). The upper-bound of λ is also limited by the biophysical model. Here, without inhibition and with an average event of 200 pS, only limited increases of λ_{max} are possible. Such limited changes have a negligible effect on mutual information. For example, a 20% increase in λ_{max} increases mutual information from 3.0 bits/spike to 3.08 bits/spike, a 2.6% increase. Going in the other direction, a 25% decrease in λ_{max} causes a 4% decrease in bits/spike.

Since we do not know the marginal probability distribution for Λ , we compare the result for three different distributions. The distributions, and each of their associated mutual information values, are summarized in Table 1. The calculations are described in the methods section.

Discussion

Here, the discussion focuses on the following results: (i) discovery of a 1/TTS relationship consistent with a specific form of linear additivity and with a specific distributional form suggested by the linear additivity, (ii) the relative effects on mutual information of thermal noise, sodium channel shot-noise, and random synaptic activations, and (iii) mutual information, for which values here are compared to another in the literature.

Linear additivity

Linear additivity is a pervasive assumption in many computational models, dating back to McCulloch and Pitts [1]; linear computation (or log-linear) is assumed, and seemingly required, for several recent computational models [44, 62, 63].

The results here show that, over a limited range of intensities, this biophysical model produces the desired inverse relationship between excitation intensity and TTS (Fig 1). Notably, this inverse proportionality occurs without manipulating the highly nonlinear biophysical parameters and specified localizations of the voltage-gated conductances, all of which were inherited from the consensus layer V pyramidal model [19, 46–49, 49, 51]. This inverse proportionality is observed for the nonstochastic, current-step injections at the soma (see S2 Fig), as well as observed for the stochastic, spatially distributed synaptic excitation. The somatic injection results suggest that the observed linearization generalizes to excitation distributed over basal dendrites, which connect to the soma. As expected, this extension is confirmed through a modest number of simulations.

Additionally, the model well approximates an inverse Gaussian (IG) distribution of the TTS (Fig 4). Indeed, this idea of the IG and the linearity required of the excitation process is quite old; a result first pointed out in neuroscience by Gerstein and Mandelbrot [2]. This linearization result is only approximately available to an Ornstein-Uhlenbeck diffusion because the approximation is good only at short time intervals [64] while the inverse linearization here is

over a range of four time constants ($\tau = 12$ ms). Empirically, at least two studies use the IG first hitting-time distribution to fit interpulse intervals using extracellular recording from intact animals [65, 66]. Moreover, one suspects the paucity of such IG fits is due to lack of trying rather than the failure of the fits themselves.

In addition to the existence of an empirically relevant biophysical model that produces the IG distributions of IPIs, such an IG fit supports the perspective of computational models that assume linear additivity of synaptic activation. That is, even though we know that the underlying biophysical processes are highly nonlinear and that this is a leaky neuron, the fits here are close to an IG. Therefore, the accumulation of internal excitation can be treated as linear additivity in the sense that an uncorrelated linearly additive continuous process hitting a straight barrier (nominal threshold) must be an IG [2, 56, 67].

On the other hand, supralinear summation has been observed neurophysiologically [31, 32]. But even in this case, the ideas advanced here may turn out to be applicable. Supralinear additivity, e.g. a time-independent but barrier-dependent interaction with voltage, can generate other first hitting-time distributions. Because first hitting-time is inversely proportional to input intensity for any member of the generalized IG class with the variance of synaptic events proportional to the intensity of events, these distributions are viable candidates for fitting models with supralinear excitation (see [S1 Text](#) for further explication). Unfortunately, in our hands, distinguishing between data-fits for appropriately parameterized IG vs. generalized IG distributions is problematic.

Studies suggesting sublinear charging of the initial segment are not consistent with our observations. A purely passive neuron (no voltage-activated channels) is a popular sublinear model that produces an Ornstein-Uhlenbeck diffusion [6–8]. Although such models are unsuitable for a passive neuron, the assumption of a purely passive neuron is somewhat dated.

In sum, the observations here serve as: (1) a prime example of complexity—the voltage-activated conductances—leading to simplicity—producing the equivalent of linear additivity of synaptic events and a closed-form probability distribution of first hitting-time; and (2) for computational models that assume IPI coding, the assumption of linear additivity is good enough, at least in terms of agreeing with a physiologically relevant, biophysical model of a neocortical neuron. In this regard, the observations of linear additivity *in vivo* [21, 26, 27] gives additional relevance to the findings here.

Sources of noise

Some recent reviews have speculated on various qualitative sources of noise [64, 68–72] that would lower the information throughput of a neuron. It is fairly well-established that random synaptic arrivals (alternatively, synaptic noise) dominates [73] and that the second-largest source of unpredictable fluctuations is ion-channel shot-noise [74–76] (as noted in [68]). In this regard, voltage-activated sodium channels are believed to be the major contributor to total channel shot-noise [77, 78]. Here, we are concerned with a precise, quantitative statement of noise in the context of the initial segment of a consensus pyramidal neuron. Historically, perhaps the earliest relevant measurement estimating noise sources is [79]; they suggest that synaptic noise can account for all the variability in IPIs. Because their observations were performed *in vivo*, their results cannot directly isolate the noise contributions from the synaptic input versus channel noise; however, the modeling-based observations here are able to do so (Fig 3). Even more recent results [73] do not contradict the idea that synaptic noise dominates over channel-noise. Although their results suggest non-Poisson inputs, their interpretations are consistent with synaptic variability dominating VAC shot-noise variability in the physiological situation. Comparing the empirical, neurophysiological study to the biophysical

model here, there is a notable difference in the duration of the excitatory inputs. In the empirical study, long-duration stimuli are used (lasting about one second) while here durations are used on the timescale of physiological IPIs. Apparently, the general conclusion of noise contributions is robust across such large differences in stimuli.

Under a very different set of assumptions, Sengupta et al. [80] also conclude that VAC shot-noise is only a minor and possibly ignorable source of input-output variability. Two distinctions stand out when comparing their results to the current study. Their model neuron is a biophysical neuron but seemingly somewhat arbitrary in its construction relative to the one studied here. Second, they model a dynamic input signal, perhaps inspired by the fly eye research. In contrast, the neuron of interest here can be thought of as performing computation (perhaps discrimination) over the interval of a visual fixation. In any case, the qualitative conclusions are the same.

While it is certainly true that noise limits the detection by peripheral sensors (hair cells in the cochlea, cones in the eye, etc.), we speculate that randomization processes are of much more concern in calculating information transmitted between neurons than explicit noise processes including thermal noise and shot noise of voltage-activated conductances. Rather than calling the unpredictable firing of a neuron 'noise', we prefer the term randomization, which is produced by the large number of poorly synchronized, input-line activations. Moreover, any such randomization process is itself enhanced by quantal synaptic failures [81].

Mutual information

For the scene analysis problem considered here, one can propose the existence of a scalar, latent random variable, Λ , and a conjectured, continuous output code [14]. With these two hypotheses, the computational and information-transmission problem concerns estimating and communicating $\Lambda = \lambda$ [45]. The input variable, λ , is a Poisson rate created by a union of the input lines, each treated as no more than a point process [82]. Thus, we assume a Poisson process as the input in calculating Shannon's mutual information.

In any calculation of mutual information, one must assume an input distribution. Our assumption arises from a model inspired by pyramidal neuron firing in V1 during a visual fixation. For this model, most of the neurons, most of the time are firing well below their maximum firing rate. Of course, transiently some neurons are receiving an input close to their best input, in which case they would be driven for 2 or 3 pulses at 200 Hz [83, 84]. The study here allows for an approximation of this range with our defined priors. Since we do not know the correct prior distribution, we evaluate three possibilities, each of which is compatible with the dynamic range of the biophysical neuron being studied. Two of these prior probability distributions (the λ^{-1} distribution and the exponential distribution) reflect the fact that the neuron hardly spends any time firing at high frequencies.

Our estimate of mutual information agrees with the approximately 3 bits per spike calculated in [85]. This distinguished calculation of mutual information uses the fly H1 model to indirectly evaluate the effect of intrinsic noise under the assumption of a continuously and rather rapidly fluctuating visual scene (at the very least, 25 Hz, and certainly with higher-order frequency components present in the visual input). Such an input is consistent with the visual stimulus of a moving fly. However, for the visual fixation problem posited here, the driving input is, on average, changing at a rate less than 10 Hz. Nevertheless, the comparative values of bit rate are, perhaps surprisingly, in agreement. More broadly, the results here also agree with a range of other estimates, from 2 – 5 bits per spike [86–93]; see [94] for a review.

It can be argued that the 3 bits calculated here are an underestimate due to the constraints imposed on the consensus neuron being used. For example, the model considered here

sustains firing only over a limited range of input intensities, and a more accurate neuron with more voltage-activated conductances (*e.g.* the I_h conductance or even a large set of spatially-distributed conductances [95, 96]) might lead to a neuron that has a greater dynamic range. Another limitation of the current study is a lack of inhibition. Physiologically, a neocortical neuron will simultaneously receive inhibition and excitation. Such inhibition downgrades the effect of synaptic events, which in turn requires larger values of Λ to produce the same firing rates. By increasing the number of synaptic events per output spike, the information rate per output spike increases. For example, a four-fold increase in the number of events needed to fire the neuron increases the mutual information by about 1 bit / spike. On the other hand, the conditional independence assumption (see [Methods](#)) might lead to a value that is inappropriately high.

Suggestions for future research

Suggestions for future research include both biophysical modeling and experimental neurophysiology. The biophysical modeling should detail the interactions, as a function of both time and voltage, between the Na^+ and K^+ channels underlying the linearized relationship investigated here. In another direction, the biophysical models should also consider adding other conductances, particularly I_h (and novel ideas about this conductance [96]). Perhaps most challenging will be incorporation of well-quantified dendritic spiking phenomena. Regarding this challenge, there are at least two perspectives that require separate consideration: (i) analysis of the far apical spike with regard to $1/\text{TTS}$ and (ii) the analysis of the union of (a) the basal dendritic spikes and (b) the spikes of the near apical dendritic branches.

Regarding empirical intracellular research, there are again two suggestions using a layer V neocortical pyramidal neuron. First, using the TTS observations as before, there is a need to extend the intensity range studied to include both higher and lower intensities leading to both shorter and longer TTSs than currently available. Second, the observations and inferences here also motivate twin-pulse excitations; that is, how does TTS vary as a function of the time since the most recent output spike? Finally, we look forward to basic TTS observations for layer 2/3 pyramidal neurons.

The work here is no more than a first step in characterizing functionality consistent with linear additivity; for example, it is restricted to only one type of neuron and the available neurophysiological observations [46, 47, 51, 52]. Whether the inverse relationship between TTS and input intensity, and therefore the viability of the linear additivity hypothesis, will occur in other pyramidal neurons remains an open question. With the advent of new constraining neurophysiological data to go along with a more detailed knowledge of the voltage-activated channels, the hypotheses raised here can be retested and modified as necessary. Hopefully, the way we have analyzed the biophysical data here will encourage neurophysiologists to measure and analyze their empirical data in a similar manner.

Methods

Model

This work models a Layer 5 pyramidal cell quantified by Mainen and Sejnowski [47] (their Fig 1D). The biophysical model evolved from [51] in which it was used to study back propagating action potential spikes. This led to [46] in which it was further refined (model can be retrieved from ModelDB [97]). The model was fit to measurements at several different places on the neuron including the AIS, axon, and dendrites.

The model includes both Nav 1.6 and Nav 1.2 channels distributed along the AIS. It is well-accepted that the action potential is initiated at the distal AIS [52, 54, 98] with its high

concentration of both sodium channel types [53, 55, 99]. The parameter sweeps of [46] (see their Fig 5) severely restrict the placement of the two types of sodium channels. The capacitance in the soma is changed from $1 \mu\text{F}/\text{cm}^2$ to $0.9 \mu\text{F}/\text{cm}^2$, as this is a more realistic value [100]. In addition, a small amount of persistent Na channels is added at the proximal apical dendrite to simulate more realistic neuronal firing over a longer range of times. The persistent sodium channels are modelled using the Nav1.6 channels with shifted inactivation rate equations, so that they would inactivate much more slowly [59, 98, 101].

The main change is the alteration of sodium channels so that they operated stochastically. The stochastic sodium channels are modeled with a widely-used eight-state kinetic reaction scheme describing the m^3h Hodgkin-Huxley activation kinetics [102, 103] quantified in [50]. This gating scheme is shown in [104] (their Fig 4A). When run deterministically, there is no variability. These changes do not noticeably change the overall shape of the action potential (Fig 5). The main difference is that the stochastic voltage-trace lies just below the deterministic trace 200–300 μs before firing. Since it is noisier, the stochastic neuron can suddenly cross threshold with a stochastic event, and thus does not consistently approach threshold in the gradual manner of the deterministic neuron. Thus, compared to the deterministic neuron, the stochastic neuron tends to be at a slightly lower voltage when it fires (see S4 Fig).

Excitation

Simulations are performed using the simulation environment NEURON [105]. All simulations are run at 37°C with a time step of $1 \mu\text{s}$, and the results do not change for smaller time steps. In all cases, the neuron is allowed to come to steady state before the stimulus is applied. The neuron is stimulated in the main apical dendrite $250 \mu\text{m}$ from the soma. For these layer V pyramidal cells, our interests center on synapses that exclude the distal tuft which we presume has its own independent computations (for example see [44, 106, 107]). Then, noting the anatomy of such layer V cells (see Fig 1A in [108] or Fig 1d in [47]), the vast majority of dendritic surface area, and therefore synaptic localizations, is within $300 \mu\text{m}$ of the cell body. That is, the cell's dendritic surface area is dominated by basal and near-apical dendritic branches whose distal tips are almost inevitably less than $300 \mu\text{m}$ from the cell body.

Stimulation is performed in two ways: first with a noise-free current-step in the main apical dendrite, and second by simulating synaptic activity. Synaptic activity is simulated using synapses distributed evenly along the main apical dendrite $200 \mu\text{m}$ – $300 \mu\text{m}$ from the soma. A small number of simulations are performed by scattering synapses on five of the basal dendrites with no differences noted from the main set of simulations. Synapses are simulated as the Poisson arrival of square pulses of 200 pS lasting 1.2 ms with a reversal potential of 0 mV . The Poisson assumption used here arises not from a Poisson assumption on individual inputs, but the Poisson approximation [109] produced by the unioning of all the input lines, each one being a point process.

The restricted range of current-step intensities begin with those of the physiological studies of Hu et al. 2009; that is, their range is the starting point upon which we expand. At very high intensities, their model tends to initiate spiking from the near apical dendrite. The physiological nature of such a dendritically originated spike remains an open question. Because there are such strong arguments for initial segment initiations [52], we postpone using this biophysical observation until neurophysiology confirms or denies its existence.

Mutual information calculation

Treating the neuron as an information channel, we identify the input random variable as Λ and the output random variable as TTS. In order to calculate the mutual information $I(\Lambda;$

TTS), we require the pair of distributional forms $P(\Lambda)$ and $P(TTS|\Lambda = \lambda)$ for all λ . $P(TTS)$ is inferred from these forms (see Eq 2) and then calculate the mutual information (see Eq 4).

P(Λ). Three distinct distributions are investigated for $P(\Lambda)$. In all cases, these distributions were assumed to have the finite range of interest here. Very low intensities of excitation that never yield a spike are of no interest because there is no IPI to decode. Likewise, extremely high intensity input, as is possible with intracellular current injection but not possible using synaptic input, is out of the range of interest. Finally, any aspects of the neuron’s voltage once threshold is closely approached and achieved is not of interest. See Table 1 for the investigated distributional forms and the associated range of Λ .

P($TTS|\Lambda$). The results suggest that at a given intensity λ , the distribution of TTS is well-approximated by an inverse Gaussian distribution (see Fig 2). The PDF of the inverse Gaussian distribution with a mean of μ and a shape parameter of ρ is (here tts is a realization of the random variable TTS):

$$IG(\mu(\lambda), \rho(\lambda)) = \left(\frac{\rho(\lambda)}{2\pi t t s^3}\right)^{1/2} \exp\left(\frac{-\rho(\lambda)t t s - \mu(\lambda)^2}{2\mu(\lambda)^2 t t s}\right) \tag{1}$$

An expression for $P(TTS|\Lambda)$ requires the parameters μ and ρ for any λ in the assumed range. Given a value of λ and eventually using sample values for population values, the mean $\mu(\lambda)$ corresponds to $E[TTS|\lambda]$ and the shape parameter $\rho(\lambda)$ corresponds to $E[TTS|\lambda]^3/Var[TTS|\lambda]$. The conditional sample mean, *c.a.* $E[TTS|\lambda]$, is approximated with a best-fit to the collected data plotting $E[TTS|\lambda]$ as a function of $1/\lambda$, and the conditional sample variance, *c.a.* $Var[TTS|\lambda]$, is approximated with a best-fit to the collected data plotting $Var[TTS|\lambda]$ as a function of $1/\lambda$. When it was necessary to extrapolate the variance beyond the range of collected data, the largest observed variance was used (18.57 ms^2). The regression generated means and variances are in S1 Table.

P(TTS). $P(TTS)$ is computed by numerical integration with Mathematica over the entire range under consideration.

$$P(TTS) = \int_{\lambda=32.8 \text{ events/ms}}^{\lambda=83.3 \text{ events/ms}} P(TTS|\Lambda = \lambda) \cdot P_{\Lambda}(\lambda) d\lambda \tag{2}$$

The resulting $P(TTS)$ distributions are shown in S3 Fig.

I(Λ ; TTS). The mutual information (in bits / spike) is given by the following double integral.

$$I(\Lambda; TTS) = \int_{\lambda=32.8 \text{ events/ms}}^{\lambda=83.3 \text{ events/ms}} P_{\Lambda}(\lambda) \int_0^{\infty} P(TTS|\lambda) \log_2 \frac{P(TTS|\Lambda = \lambda)}{P(TTS)} dt t s d\lambda \tag{3}$$

This double integral is approximated using the following equation by summing over Λ with steps of 0.1 events/ms and by summing over TTS in the range [1 ms, 250 ms] with steps of 0.05 ms. Decreasing this step size by half does not change the value of the summation.

$$I(\Lambda; TTS) = \sum_{\lambda=32.8 \text{ events/ms}}^{\lambda=83.3 \text{ events/ms}} P_{\Lambda}(\lambda) \sum_{1 \text{ ms}}^{250 \text{ ms}} P(TTS|\lambda) \log_2 \frac{P(TTS|\Lambda = \lambda)}{P(TTS)} \tag{4}$$

The mutual information calculation assumes independence between successive values of the latent variables.

Supporting information

S1 Fig. Mutual information values over different extrapolated ranges. All calculations share the same shortest TTS (6.8 ms) and use the same distributional form for Λ (c/λ , where c is a constant). The maximum value of λ is 83.33 events/ms. The minimum value of λ changes depending upon the longest TTS in the range, and the value of c is chosen to normalize the distribution.

(EPS)

S2 Fig. A linear inverse TTS as a function of somatic excitation. Excitation is a point current-step in the soma. The dashed line is a best linear fit. Each point is an average of 120 excitations from rest. The error bars (SEM) for the current-step are within the plot points. All points have spike initiation at the AIS.

(EPS)

S1 Text.

(PDF)

S1 Table. Values for discrete intensity steps and the corresponding sample statistics.

(PDF)

S3 Fig. $P(TTS)$ distributions. (A) The $P(TTS)$ distribution (thick blue curve) is computed as the weighted sum of conditional distributions. Conditional distributions, $P(TTS|\lambda)$, are shown for $\lambda = 80$ events/ms (red dashed line), $\lambda = 50$ events/ms (green dotted line), and $\lambda = 40$ events/ms (thin black line). (B) The resulting discrete $P(TTS)$ distributions (approximating the continuous densities) implied by the three different Λ distributions of [Table 1](#).

(EPS)

S4 Fig. Voltage traces responding to a current-step and stochastic synaptic-step. Voltage is measured at the AIS. The current-step is 0.7 nA, and the stochastic synaptic step is 58.33 events/ms. Although the average input current is the same, the action potential evoked by the stochastic conductance step is, in general, later than the action potential evoked by the current step (see histograms in [Fig 5](#)) This delay occurs because the synaptic conductance events are distributed over a 100 μm section of the apical dendrite while the current-step is a point source in this dendrite.

(EPS)

Acknowledgments

We thank Costa Colbert for helpful suggestions and comments during the research and the writing of the manuscript. We thank the Department of Neurosurgery for their financial support and also are thankful for the US National Science Foundation Grant 1162449 – Toby Berger, PI.

Author Contributions

Conceptualization: William B. Levy.

Data curation: Chandan Singh.

Formal analysis: Chandan Singh, William B. Levy.

Investigation: Chandan Singh, William B. Levy.

Methodology: William B. Levy.

Software: Chandan Singh.

Supervision: William B. Levy.

Visualization: Chandan Singh, William B. Levy.

Writing – original draft: Chandan Singh, William B. Levy.

Writing – review & editing: Chandan Singh, William B. Levy.

References

1. McCulloch WS, Pitts W. A logical calculus of the ideas immanent in nervous activity. *The bulletin of mathematical biophysics*. 1943; 5(4):115–133. <https://doi.org/10.1007/BF02478259>
2. Gerstein GL, Mandelbrot B. Random walk models for the spike activity of a single neuron. *Biophysical journal*. 1964; 4(1 Pt 1):41. [https://doi.org/10.1016/S0006-3495\(64\)86768-0](https://doi.org/10.1016/S0006-3495(64)86768-0) PMID: 14104072
3. Bernander O, Koch C, Douglas RJ. Amplification and linearization of distal synaptic input to cortical pyramidal cells. *Journal of neurophysiology*. 1994; 72(6):2743–2753. PMID: 7897486
4. Morel D, Levy WB. Persistent sodium is a better linearizing mechanism than the hyperpolarization-activated current. *Neurocomputing*. 2007; 70(10):1635–1639. <https://doi.org/10.1016/j.neucom.2006.10.054>
5. Morel D, Levy WB. Cost of linearization for different time constants. *BMC Neuroscience*. 2008; 9(1):1.
6. Ricciardi LM, Sacerdote L. The Ornstein-Uhlenbeck process as a model for neuronal activity. *Biological cybernetics*. 1979; 35(1):1–9. <https://doi.org/10.1007/BF01845839> PMID: 508846
7. Giorno V, Lánský P, Nobile A, Ricciardi L. Diffusion approximation and first-passage-time problem for a model neuron. *Biological cybernetics*. 1988; 58(6):387–404. <https://doi.org/10.1007/BF00361346> PMID: 3395633
8. Capocelli R, Ricciardi L. Diffusion approximation and first passage time problem for a model neuron. *Kybernetik*. 1971; 8(6):214–223. <https://doi.org/10.1007/BF00288750> PMID: 5090384
9. Lánský P, Rospars JP. Ornstein-Uhlenbeck model neuron revisited. *Biological cybernetics*. 1995; 72(5):397–406. <https://doi.org/10.1007/BF00201415>
10. Lánský P, Sacerdote L. The Ornstein-Uhlenbeck neuronal model with signal-dependent noise. *Physics Letters A*. 2001; 285(3):132–140.
11. Lansky P, Smith C, Ricciardi LM. One-dimensional stochastic diffusion models of neuronal activity and related first passage time problems. *Trends in Biological Cybernetics*. 1990; 1:153–162.
12. Stein RB. A theoretical analysis of neuronal variability. *Biophysical Journal*. 1965; 5(2):173. [https://doi.org/10.1016/S0006-3495\(65\)86709-1](https://doi.org/10.1016/S0006-3495(65)86709-1) PMID: 14268952
13. Tuckwell HC, Ditlevsen S. The space-clamped Hodgkin-Huxley system with random synaptic input: inhibition of spiking by weak noise and analysis with moment equations. *arXiv preprint arXiv:160404796*. 2016;.
14. Berger T, Levy WB. A mathematical theory of energy efficient neural computation and communication. *IEEE Transactions on Information Theory*. 2010; 56(2):852–874. <https://doi.org/10.1109/TIT.2009.2037089>
15. McDonnell MD, Ikeda S, Manton JH. An introductory review of information theory in the context of computational neuroscience. *Biological cybernetics*. 2011; 105(1):55–70. <https://doi.org/10.1007/s00422-011-0451-9> PMID: 21792610
16. Xing J, Berger T, Sejnowski TJ. A Berger-Levy energy efficient neuron model with unequal synaptic weights. In: *Information Theory Proceedings (ISIT), 2012 IEEE International Symposium on*. IEEE; 2012. p. 2964–2968.
17. Sungkar M, Berger T, Levy WB. Mutual Information and Parameter Estimation in the Generalized Inverse Gaussian Diffusion Model of Cortical Neurons. *IEEE Transactions on Molecular, Biological and Multi-Scale Communications*. 2016; 2(2):166–182. <https://doi.org/10.1109/TMBMC.2017.2656861>
18. Izhikevich EM, et al. Simple model of spiking neurons. *IEEE Transactions on neural networks*. 2003; 14(6):1569–1572. <https://doi.org/10.1109/TNN.2003.820440> PMID: 18244602
19. Acker CD, Antic SD. Quantitative assessment of the distributions of membrane conductances involved in action potential backpropagation along basal dendrites. *Journal of neurophysiology*. 2009; 101(3):1524–1541. <https://doi.org/10.1152/jn.00651.2007> PMID: 19118105

20. Ermentrout GB, Terman DH. *Mathematical foundations of neuroscience*. vol. 35. Springer Science & Business Media; 2010.
21. Ferster D. Linearity of synaptic interactions in the assembly of receptive fields in cat visual cortex. *Current opinion in neurobiology*. 1994; 4(4):563–568. [https://doi.org/10.1016/0959-4388\(94\)90058-2](https://doi.org/10.1016/0959-4388(94)90058-2) PMID: 7812146
22. Carandini M, Ferster D. Membrane potential and firing rate in cat primary visual cortex. *The Journal of Neuroscience*. 2000; 20(1):470–484. PMID: 10627623
23. Gillespie DC, Lampl I, Anderson JS, Ferster D. Dynamics of the orientation-tuned membrane potential response in cat primary visual cortex. *Nature neuroscience*. 2001; 4(10):1014–1019. <https://doi.org/10.1038/nn731> PMID: 11559853
24. Jagadeesh B, Wheat HS, Ferster D. Linearity of summation of synaptic potentials underlying direction selectivity in simple cells of the cat visual cortex. *Science-AAAS-Weekly Paper Edition-including Guide to Scientific Information*. 1993; 262(5141):1901–1905.
25. Priebe NJ, Ferster D. Direction selectivity of excitation and inhibition in simple cells of the cat primary visual cortex. *Neuron*. 2005; 45(1):133–145. <https://doi.org/10.1016/j.neuron.2004.12.024> PMID: 15629708
26. Léger JF, Stern EA, Aertsen A, Heck D. Synaptic integration in rat frontal cortex shaped by network activity. *Journal of neurophysiology*. 2005; 93(1):281–293. PMID: 15306631
27. Carandini M, Heeger DJ, Movshon JA. Linearity and normalization in simple cells of the macaque primary visual cortex. *Journal of Neuroscience*. 1997; 17(21):8621–8644. PMID: 9334433
28. Cash S, Yuste R. Input summation by cultured pyramidal neurons is linear and position-independent. *The Journal of neuroscience*. 1998; 18(1):10–15. PMID: 9412481
29. Cash S, Yuste R. Linear summation of excitatory inputs by CA1 pyramidal neurons. *Neuron*. 1999; 22(2):383–394. [https://doi.org/10.1016/S0896-6273\(00\)81098-3](https://doi.org/10.1016/S0896-6273(00)81098-3) PMID: 10069343
30. Araya R, Eiselthel KB, Yuste R. Dendritic spines linearize the summation of excitatory potentials. *Proceedings of the National Academy of Sciences*. 2006; 103(49):18799–18804. <https://doi.org/10.1073/pnas.0609225103>
31. Nettleton JS, Spain WJ. Linear to supralinear summation of AMPA-mediated EPSPs in neocortical pyramidal neurons. *Journal of Neurophysiology*. 2000; 83(6):3310–3322. PMID: 10848551
32. Cook EP, Wilhelm AC, Guest JA, Liang Y, Masse NY, Colbert CM. The neuronal transfer function: contributions from voltage-and time-dependent mechanisms. *Progress in brain research*. 2007; 165:1–12. [https://doi.org/10.1016/S0079-6123\(06\)65001-2](https://doi.org/10.1016/S0079-6123(06)65001-2) PMID: 17925236
33. Sparks D. Population coding of saccadic eye movements by neurons in the superior colliculus. *Nature*. 1988; 332:357–360. <https://doi.org/10.1038/332357a0> PMID: 3352733
34. Sompolinsky H, Yoon H, Kang K, Shamir M. Population coding in neuronal systems with correlated noise. *Physical Review E*. 2001; 64(5):051904. <https://doi.org/10.1103/PhysRevE.64.051904>
35. Woolley SM, Gill PR, Theunissen FE. Stimulus-dependent auditory tuning results in synchronous population coding of vocalizations in the songbird midbrain. *The Journal of Neuroscience*. 2006; 26(9):2499–2512. <https://doi.org/10.1523/JNEUROSCI.3731-05.2006> PMID: 16510728
36. Tripathy SJ, Padmanabhan K, Gerkin RC, Urban NN. Intermediate intrinsic diversity enhances neural population coding. *Proceedings of the National Academy of Sciences*. 2013; 110(20):8248–8253. <https://doi.org/10.1073/pnas.1221214110>
37. Chikazoe J, Lee DH, Kriegeskorte N, Anderson AK. Population coding of affect across stimuli, modalities and individuals. *Nature neuroscience*. 2014; 17(8):1114–1122. <https://doi.org/10.1038/nn.3749> PMID: 24952643
38. Barak O, Tsodyks M, Romo R. Neuronal population coding of parametric working memory. *The Journal of Neuroscience*. 2010; 30(28):9424–9430. <https://doi.org/10.1523/JNEUROSCI.1875-10.2010> PMID: 20631171
39. Averbeck BB, Latham PE, Pouget A. Neural correlations, population coding and computation. *Nature Reviews Neuroscience*. 2006; 7(5):358–366. <https://doi.org/10.1038/nrn1888> PMID: 16760916
40. Gerwin S, Macke JH, Bethge M. Bayesian inference for generalized linear models for spiking neurons. *Frontiers in Computational Neuroscience*. 2010; 4(12). <https://doi.org/10.3389/fncom.2010.00012> PMID: 20577627
41. Deneve S. Bayesian spiking neurons I: inference. *Neural computation*. 2008; 20(1):91–117. PMID: 18045002
42. Ma WJ, Beck JM, Latham PE, Pouget A. Bayesian inference with probabilistic population codes. *Nature neuroscience*. 2006; 9(11):1432–1438. <https://doi.org/10.1038/nn1790> PMID: 17057707

43. Beck JM, Ma WJ, Kiani R, Hanks T, Churchland AK, Roitman J, et al. Probabilistic population codes for Bayesian decision making. *Neuron*. 2008; 60(6):1142–1152. <https://doi.org/10.1016/j.neuron.2008.09.021> PMID: 19109917
44. Levy WB, Colbert CM, Desmond NL. *Elemental adaptive processes of neurons and synapses: a statistical/computational perspective*. vol. 187. Erlbaum, Hillsdale, NJ; 1990.
45. Levy WB, Berger T, Sungkar M. Neural Computation From First Principles: Using the Maximum Entropy Method to Obtain an Optimal Bits-Per-Joule Neuron. *T-MBMC*. 2016; 2:154–165.
46. Hu W, Tian C, Li T, Yang M, Hou H, Shu Y. Distinct contributions of Nav1. 6 and Nav1. 2 in action potential initiation and backpropagation. *Nature neuroscience*. 2009; 12(8):996–1002. <https://doi.org/10.1038/nn.2359> PMID: 19633666
47. Mainen ZF, Sejnowski TJ, et al. Influence of dendritic structure on firing pattern in model neocortical neurons. *Nature*. 1996; 382(6589):363–366. <https://doi.org/10.1038/382363a0> PMID: 8684467
48. Hallermann S, de Kock CP, Stuart GJ, Kole MH. State and location dependence of action potential metabolic cost in cortical pyramidal neurons. *Nature neuroscience*. 2012; 15(7):1007–1014. <https://doi.org/10.1038/nn.3132> PMID: 22660478
49. Banitt Y, Martin KA, Segev I. A biologically realistic model of contrast invariant orientation tuning by thalamocortical synaptic depression. *The Journal of Neuroscience*. 2007; 27(38):10230–10239. <https://doi.org/10.1523/JNEUROSCI.1640-07.2007> PMID: 17881529
50. Kole MH, Hallermann S, Stuart GJ. Single Ih channels in pyramidal neuron dendrites: properties, distribution, and impact on action potential output. *The Journal of neuroscience*. 2006; 26(6):1677–1687. <https://doi.org/10.1523/JNEUROSCI.3664-05.2006> PMID: 16467515
51. Yu Y, Shu Y, McCormick DA. Cortical action potential backpropagation explains spike threshold variability and rapid-onset kinetics. *The Journal of Neuroscience*. 2008; 28(29):7260–7272. <https://doi.org/10.1523/JNEUROSCI.1613-08.2008> PMID: 18632930
52. Baranauskas G, David Y, Fleidervish IA. Spatial mismatch between the Na⁺ flux and spike initiation in axon initial segment. *Proceedings of the National Academy of Sciences*. 2013; 110(10):4051–4056. <https://doi.org/10.1073/pnas.1215125110>
53. Kole MH, Ilschner SU, Kampa BM, Williams SR, Ruben PC, Stuart GJ. Action potential generation requires a high sodium channel density in the axon initial segment. *Nature neuroscience*. 2008; 11(2):178–186. <https://doi.org/10.1038/nn2040> PMID: 18204443
54. Johnston D, Magee JC, Colbert CM, Christie BR. Active properties of neuronal dendrites. *Annual review of neuroscience*. 1996; 19(1):165–186. <https://doi.org/10.1146/annurev.ne.19.030196.001121> PMID: 8833440
55. Colbert CM, Pan E. Ion channel properties underlying axonal action potential initiation in pyramidal neurons. *Nature neuroscience*. 2002; 5(6):533–538. <https://doi.org/10.1038/nn0602-857> PMID: 11992119
56. Schrodinger E. *Statistical Thermodynamics*. Statistical Thermodynamics, by Schrodinger Erwin, Cambridge, UK: Cambridge University Press, 1968. 1968;1.
57. Andrásfalvy BK, Magee JC. Changes in AMPA receptor currents following LTP induction on rat CA1 pyramidal neurones. *The Journal of physiology*. 2004; 559(2):543–554. <https://doi.org/10.1113/jphysiol.2004.065219> PMID: 15235093
58. Conti F, Hille B, Neumcke B, Nonner W, Stämpfli R. Measurement of the conductance of the sodium channel from current fluctuations at the node of Ranvier. *The Journal of physiology*. 1976; 262(3):699–727. <https://doi.org/10.1113/jphysiol.1976.sp011616> PMID: 1087643
59. Chatelier A, Zhao J, Bois P, Chahine M. Biophysical characterisation of the persistent sodium current of the Nav1. 6 neuronal sodium channel: a single-channel analysis. *Pflügers Archiv-European Journal of Physiology*. 2010; 460(1):77–86. <https://doi.org/10.1007/s00424-010-0801-9> PMID: 20204400
60. Papoulis A, Pillai SU. *Probability, Random Variables, and Stochastic Processes*. Probability, Random Variables, and Stochastic Processes, Fourth Edition, by Papoulis Athanasios and Pillai S Unnikrishna ISBN 978-0-07-366011-0 Published by McGraw-Hill Higher Education (a division of McGraw-Hill Companies), New York, NY USA, 2002. 2002;1.
61. Lindley DV. On a measure of the information provided by an experiment. *The Annals of Mathematical Statistics*. 1956;p. 986–1005. <https://doi.org/10.1214/aoms/1177728069>
62. Deneve S, Pouget A. Bayesian multisensory integration and cross-modal spatial links. *Journal of Physiology-Paris*. 2004; 98(1):249–258. <https://doi.org/10.1016/j.jphysparis.2004.03.011>
63. Barber MJ, Clark JW, Anderson CH. Neural representation of probabilistic information. *Neural Computation*. 2003; 15(8):1843–1864. <https://doi.org/10.1162/08997660360675062> PMID: 14511515

64. Simen P, Balci F, Cohen JD, Holmes P, et al. A model of interval timing by neural integration. *The Journal of Neuroscience*. 2011; 31(25):9238–9253. <https://doi.org/10.1523/JNEUROSCI.3121-10.2011> PMID: 21697374
65. Iyengar S, Liao Q. Modeling neural activity using the generalized inverse Gaussian distribution. *Biological Cybernetics*. 1997; 77(4):289–295. <https://doi.org/10.1007/s004220050390> PMID: 9394447
66. Brown EN, Barbieri R, Ventura V, Kass RE, Frank LM. The time-rescaling theorem and its application to neural spike train data analysis. *Neural computation*. 2002; 14(2):325–346. <https://doi.org/10.1162/08997660252741149> PMID: 11802915
67. Wald A. *Sequential analysis*. Courier Corporation; 1973.
68. Faisal AA, Selen LP, Wolpert DM. Noise in the nervous system. *Nature reviews neuroscience*. 2008; 9(4):292–303. <https://doi.org/10.1038/nrn2258> PMID: 18319728
69. Tuckwell HC. *Introduction to theoretical neurobiology: volume 2, nonlinear and stochastic theories*. vol. 8. Cambridge University Press; 2005.
70. Yarom Y, Hounsgaard J. Voltage fluctuations in neurons: signal or noise? *Physiological reviews*. 2011; 91(3):917–929. <https://doi.org/10.1152/physrev.00019.2010> PMID: 21742791
71. Stein RB, Gossen ER, Jones KE. Neuronal variability: noise or part of the signal? *Nature Reviews Neuroscience*. 2005; 6(5):389–397. <https://doi.org/10.1038/nrn1668> PMID: 15861181
72. Faisal AA. Noise in neurons and other constraints. In: *Computational Systems Neurobiology*. Springer; 2012. p. 227–257.
73. Stevens CF, Zador AM. Input synchrony and the irregular firing of cortical neurons. *Nature neuroscience*. 1998; 1(3):210–217. <https://doi.org/10.1038/659> PMID: 10195145
74. Steinmetz PN, Manwani A, Koch C, London M, Segev I. Subthreshold voltage noise due to channel fluctuations in active neuronal membranes. *Journal of computational neuroscience*. 2000; 9(2):133–148. <https://doi.org/10.1023/A:1008967807741> PMID: 11030518
75. Van Rossum M, O'Brien BJ, Smith RG. Effects of noise on the spike timing precision of retinal ganglion cells. *Journal of neurophysiology*. 2003; 89(5):2406–2419. <https://doi.org/10.1152/jn.01106.2002> PMID: 12740401
76. White JA, Rubinstein JT, Kay AR. Channel noise in neurons. *Trends in neurosciences*. 2000; 23(3):131–137. [https://doi.org/10.1016/S0166-2236\(99\)01521-0](https://doi.org/10.1016/S0166-2236(99)01521-0) PMID: 10675918
77. Faisal AA, Laughlin SB. Stochastic simulations on the reliability of action potential propagation in thin axons. *PLoS Comput Biol*. 2007; 3(5):e79. <https://doi.org/10.1371/journal.pcbi.0030079> PMID: 17480115
78. Schneidman E, Freedman B, Segev I. Ion channel stochasticity may be critical in determining the reliability and precision of spike timing. *Neural computation*. 1998; 10(7):1679–1703. <https://doi.org/10.1162/089976698300017089> PMID: 9744892
79. Calvin WH, Stevens CF. Synaptic noise and other sources of randomness in motoneuron interspike intervals. *J Neurophysiol*. 1968; 31(4):574–587. PMID: 5709873
80. Sengupta B, Laughlin SB, Niven JE. Consequences of converting graded to action potentials upon neural information coding and energy efficiency. *PLoS Comput Biol*. 2014; 10(1):e1003439. <https://doi.org/10.1371/journal.pcbi.1003439> PMID: 24465197
81. Levy WB, Baxter RA. Energy-efficient neuronal computation via quantal synaptic failures. *The Journal of Neuroscience*. 2002; 22(11):4746–4755. PMID: 12040082
82. Chen LH. Poisson approximation for dependent trials. *The Annals of Probability*. 1975;p. 534–545. <https://doi.org/10.1214/aop/1176996359>
83. Roelfsema PR, Lamme VA, Spekreijse H. Object-based attention in the primary visual cortex of the macaque monkey. *Nature*. 1998; 395(6700):376–381. <https://doi.org/10.1038/26475> PMID: 9759726
84. Sugihara T, Qiu FT, von der Heydt R. The speed of context integration in the visual cortex. *Journal of neurophysiology*. 2011; 106(1):374–385. <https://doi.org/10.1152/jn.00928.2010> PMID: 21543756
85. Bialek W, Rieke F, De Ruyter Van Steveninck RR, Warland D. Reading a neural code. *Science*. 1991; 252(5014):1854–1857. <https://doi.org/10.1126/science.2063199> PMID: 2063199
86. Buracas GT, Zador AM, DeWeese MR, Albright TD. Efficient discrimination of temporal patterns by motion-sensitive neurons in primate visual cortex. *Neuron*. 1998; 20(5):959–969. [https://doi.org/10.1016/S0896-6273\(00\)80477-8](https://doi.org/10.1016/S0896-6273(00)80477-8) PMID: 9620700
87. Berry MJ, Meister M. Refractoriness and neural precision. *The Journal of Neuroscience*. 1998; 18(6):2200–2211. PMID: 9482804
88. Rieke F, Warland D, Bialek W. Coding efficiency and information rates in sensory neurons. *EPL (Europhysics Letters)*. 1993; 22(2):151. <https://doi.org/10.1209/0295-5075/22/2/013>

89. Rieke F, Bodnar D, Bialek W. Naturalistic stimuli increase the rate and efficiency of information transmission by primary auditory afferents. *Proceedings of the Royal Society of London B: Biological Sciences*. 1995; 262(1365):259–265. <https://doi.org/10.1098/rspb.1995.0204>
90. Reinagel P, Reid R. Visual stimulus statistics and the reliability of spike timing in the LGN. In: *Soc Neurosci Abstr*. vol. 24; 1998. p. 139.
91. Strong SP, Koberle R, van Steveninck RRdR, Bialek W. Entropy and information in neural spike trains. *Physical review letters*. 1998; 80(1):197. <https://doi.org/10.1103/PhysRevLett.80.197>
92. Warland DK. *Reading Between the Spikes: Real-Time Signal Processing in Neural Systems*. 1991;.
93. Warland DK, Reinagel P, Meister M. Decoding visual information from a population of retinal ganglion cells. *Journal of Neurophysiology*. 1997; 78(5):2336–2350. PMID: [9356386](https://pubmed.ncbi.nlm.nih.gov/9356386/)
94. Rieke F, Warland D, Bialek W. *Rob de Ruyter van Steveninck, Spikes, Exploring the Neural Code*. 1997;.
95. Bahl A, Stemmler MB, Herz AV, Roth A. Automated optimization of a reduced layer 5 pyramidal cell model based on experimental data. *Journal of neuroscience methods*. 2012; 210(1):22–34. <https://doi.org/10.1016/j.jneumeth.2012.04.006> PMID: [22524993](https://pubmed.ncbi.nlm.nih.gov/22524993/)
96. Revah O, Libman L, Fleidervish IA, Gutnick MJ. The Outwardly Rectifying Current of Layer 5 Neocortical Neurons that was Originally Identified as “Non-Specific Cationic” Is Essentially a Potassium Current. *PLoS one*. 2015; 10(7):e0132108. <https://doi.org/10.1371/journal.pone.0132108> PMID: [26197082](https://pubmed.ncbi.nlm.nih.gov/26197082/)
97. Hines ML, Morse T, Migliore M, Carnevale NT, Shepherd GM. ModelDB: a database to support computational neuroscience. *Journal of computational neuroscience*. 2004; 17(1):7–11. <https://doi.org/10.1023/B:JCNS.0000023869.22017.2e> PMID: [15218350](https://pubmed.ncbi.nlm.nih.gov/15218350/)
98. Palmer LM, Stuart GJ. Site of action potential initiation in layer 5 pyramidal neurons. *The Journal of neuroscience*. 2006; 26(6):1854–1863. <https://doi.org/10.1523/JNEUROSCI.4812-05.2006> PMID: [16467534](https://pubmed.ncbi.nlm.nih.gov/16467534/)
99. Royeck M, Horstmann MT, Remy S, Reitze M, Yaari Y, Beck H. Role of axonal NaV1.6 sodium channels in action potential initiation of CA1 pyramidal neurons. *Journal of neurophysiology*. 2008; 100(4):2361–2380. <https://doi.org/10.1152/jn.90332.2008> PMID: [18650312](https://pubmed.ncbi.nlm.nih.gov/18650312/)
100. Gentet LJ, Stuart GJ, Clements JD. Direct measurement of specific membrane capacitance in neurons. *Biophysical Journal*. 2000; 79(1):314–320. [https://doi.org/10.1016/S0006-3495\(00\)76293-X](https://doi.org/10.1016/S0006-3495(00)76293-X) PMID: [10866957](https://pubmed.ncbi.nlm.nih.gov/10866957/)
101. Rotaru DC, Lewis DA, Gonzalez-Burgos G. Dopamine D1 receptor activation regulates sodium channel-dependent EPSP amplification in rat prefrontal cortex pyramidal neurons. *The Journal of physiology*. 2007; 581(3):981–1000. <https://doi.org/10.1113/jphysiol.2007.130864> PMID: [17395630](https://pubmed.ncbi.nlm.nih.gov/17395630/)
102. Hille B. Ionic channels in excitable membranes. *Current problems and biophysical approaches*. *Biophysical Journal*. 1978; 22(2):283. [https://doi.org/10.1016/S0006-3495\(78\)85489-7](https://doi.org/10.1016/S0006-3495(78)85489-7) PMID: [656545](https://pubmed.ncbi.nlm.nih.gov/656545/)
103. Hille B, et al. *Ion channels of excitable membranes*. vol. 507; 2001.
104. Schmidt-Hieber C, Bischofberger J. Fast sodium channel gating supports localized and efficient axonal action potential initiation. *The Journal of Neuroscience*. 2010; 30(30):10233–10242. <https://doi.org/10.1523/JNEUROSCI.6335-09.2010> PMID: [20668206](https://pubmed.ncbi.nlm.nih.gov/20668206/)
105. Carnevale NT, Hines ML. *The NEURON book*. Cambridge University Press; 2006.
106. Levy W. A theory of the hippocampus based on reinforced synaptic modification in CA1. In: *Society for Neuroscience Abstracts*. vol. 14; 1988. p. 168.
107. Colbert CM, Levy WB. Electrophysiological and pharmacological characterization of perforant path synapses in CA1: mediation by glutamate receptors. *Journal of neurophysiology*. 1992; 68(1):1–8. PMID: [1355524](https://pubmed.ncbi.nlm.nih.gov/1355524/)
108. Mainen ZF, Sejnowski TJ. Reliability of spike timing in neocortical neurons. *Science*. 1995; 268(5216):1503. <https://doi.org/10.1126/science.7770778> PMID: [7770778](https://pubmed.ncbi.nlm.nih.gov/7770778/)
109. Barbour AD, Holst L, Janson S. *Poisson approximation*. Clarendon Press Oxford; 1992.